33RD CONGRESS
OF THE INTERNATIONAL COUNCIL
OF THE AERONAUTICAL SCIENCES
STOCKHOLM, SWEDEN, 4-9 SEPTEMBER, 2022

ICAS 2022 SWEDEN

INVESTIGATION ON CORRECTION OF TUNNEL WALL INTERFERENCE FOR DYNAMIC AIRFOIL TEST IN LOW-SPEED WIND TUNNEL

Yuqin JIAO[1], Hongyi ZOU[1], Bihua CHEN[1], Chunsheng XIAO[1]

[1]School of Aeronautics，Northwestern Polytechnical University，Xi'an 710072，China

Abstract

The dynamic airfoil wind tunnel test is a very important technical method to obtain the dynamic aerodynamic performance of the airfoil. In the dynamic airfoil wind tunnel test, the wall interference has a great influence on the accuracy of the test data. However, so far, there is no reliable and effective technical means for the correction of the wall interference in the dynamic test of airfoil in the wind tunnel, and it is necessary to carry out corresponding research. In this paper, the research on the assessment and correction of the wall interference of the dynamic airfoil test is carried out. Firstly, the experimental method of wall interference correction of dynamic airfoil wind tunnel test is studied. Using a set of NACA0012 models with different sizes, the dynamic airfoil low-speed pressure measuring test was carried out in the NF-3 low-speed wind tunnel of Northwestern Polytechnical University. The dynamic aerodynamic performance result of 0mm scale is obtained by linearly interpolation of the model test results of different scales under the same dimensionless dynamic parameters, and the wall interference of the dynamic wind tunnel test result is evaluated and corrected. The results show that the wall interference correction method can meet the actual needs, and the obtained wall interference correction amount is reasonable. Secondly, a numerical simulation correction method of wall interference for dynamic airfoil wind tunnel test is proposed. The pitch oscillation motion of the NACA0012 airfoil is taken as the research object, the numerical simulation of the flow around the airfoil model is carried out based on the motion chimera grid method. By changing the boundary conditions, the free stream around airfoil and flow in the wind tunnel are numerically simulated respectively, and the difference between the aerodynamic force and moment results of airfoil at two flow conditions can be obtained. This difference is just wall interference. The results show that the wall interference obtained by this numerical simulation method is reasonable and correct. This correction method can realize the evaluation and correction of wall interference of the unsteady airfoil test, which has the characteristics of high accuracy and easy implementation.

Keywords: Airfoil; Dynamic experiment; Correction of wall interference; Numerical simulation; Experiment

1. Introduction

The aerodynamic problem of helicopter rotors is more complicated than that of fixed-wing aircraft. The dynamic characteristics of the rotor are not only related to the aerodynamic performance of the helicopter, but also to the maneuverability and safety of the helicopter. Therefore, the study of dynamic characteristics is of great significance to the advanced rotor airfoil and blade design and the improvement of helicopter performance [1]. At present, wind tunnel testing is still a reliable means of obtaining the dynamic characteristics of the rotor airfoil. However, in a wind tunnel, the presence of the wind tunnel walls causes the aerodynamic measurements made on the model to be different from those made when the fluid boundary is infinite. This difference is called wall interference [2]. Airflow distortions around the test model induced by wind tunnel wall cause increases or decreases in drag, lift, and pitching moments that do not exist in the free atmosphere, and necessary corrections must be made before these data can be used in engineering design [3] . Compared with static tests, airfoil dynamic tests are more complex and time-dependent [4]. In the airfoil dynamic wind tunnel test, the tunnel wall interference has a great influence on the accuracy of the test data. Because the acoustic interference propagating from the airfoil surface will be

reflected back from the wind tunnel wall, and the resulting interaction can significantly affect the magnitude and phase of the airfoil aerodynamic force [5]. At present, there is no reliable and effective evaluation and correction technical means for the tunnel wall interference in dynamic wind tunnel test, and it is necessary to carry out corresponding research. In the past century, many scholars all over the world have studied the problem of unsteady aerodynamic loads, but only limited theories can be used to evaluate the effect of unsteady wall interference. Theodorsen [6] derived explicit expressions for the forces and moments on an oscillating plate in an incompressible flow in both the frequency and time domains, and expressed them as Bessel functions, and Leishman [7] further detailed the application of the method. Possio et al. [8] derived an integral equation that relates the downwash and pressure distribution of subsonic compressible flow. However, these two methods are only suitable for unbounded free flow. For the presence of wind tunnel walls, Bland[9] et al. proposed a complete solution of the linearized potential flow equation around the oscillating airfoil using the integral transformation technique under the assumption of small interference. Then, Fromme and Golberg [10] et al. extended Brand's results to more accurate mathematical calculations by improving the kernel function. However, these theories have not been tested at high angles of attack.

Ding K and Zhang W [11], et al. studied the influence of unsteady wall interference on the surface pressure of the delta wing. Huang D and Li Z [12], et al. studied the balance force measurement results of the delta wing caused by the unsteady wall interference and the influence of wall pressure. Li G, Zhang W [13] , et al. proposed an angle of attack correction method based on the surface element method, but the deviation is large in the nonlinear section.

In this paper, we investigate the evaluation and correction of wall interferences in airfoil dynamic tests using two methods. First, a group of NACA0012 models with similar geometry and different sizes are used to conduct unsteady tunnel experiments for wall interference correction. The surface pressure of the model is measured in the airfoil dynamic pressure test, and a series of data processing is performed on the pressure to obtain the corresponding lift, drag and pitching moment coefficient. The model test results are linearly interpolated to evaluate and correct for unsteady wall interferences. Second, based on the numerical simulation method of viscous flow in moving oversetting meshes, this paper proposes an evaluation and correction method for the wall interference of airfoil unsteady wind tunnel.

2. Experiment Research

2.1 Test models and equipment

The experimental research was carried out in the two dimensional test section of the NF-3 low-speed wind tunnel in School of Aeronautics of Northwestern Polytechnical University. The two-dimensional test section is 1.6 meters wide, 3 meters high and 8 meters long. The stable wind speed range is 20m/s~130m/s, and the turbulence intensity is 0.045%.

The experimental model is the NACA0012 airfoil model with mix structure of steel and wood. The chord lengths of the three geometrically similar airfoil models are 500 mm, 700 mm and 900 mm, respectively. The span-wise length is 1.6 meters, and the relative thickness of the airfoil is 12%. It can perform sinusoidal pitching oscillation along the quarter-chord point of airfoil under the drive of the driving system. Thirty-two dynamic pressure sensor mounting holes are machined along the upper and lower surfaces of each airfoil model at the center of the wingspan.

The signals of the dynamic pressure and angle sensors on the surface of the airfoil model were collected by the American Agilent VXI data acquisition system, which model is E8401A. The system has 48 measurement channels, the acquisition speed is 100kHz per channel, and it has 16-bit independent A/D converters, each channel is independently sampled in parallel. The input signal range is ±12.5mV～±10.0V, the signal range of each channel can be set independently, and the dynamic measurement accuracy is better than 0.1%FS.

The airfoil model motion drive mechanism of the NF-3 low-speed wind tunnel of Northwestern Polytechnical University uses four DDM motors to form the motion with two degrees of freedoms, that is, pitching oscillation motion and heaving motion. The overall scheme is shown in Figure 1. The same two sets of mechanisms are installed on the upper and lower walls of the wind tunnel respectively, and the output shafts of the two pitching motors are respectively connected with the two ends of the rotating shaft of the airfoil model. A linear bearing for every mechanism is installed in the vertical direction along the axis of the wind tunnel, and a sliding mechanism is installed on the linear bearings. A pitch motor is installed on the slide plate. The output shaft of the motor is perpendicular to the plane of the slide plate, and extends into the wind tunnel through the slot opened by the turntable. The slide plate can heave driven by DDM motor on the wind tunnel wall.

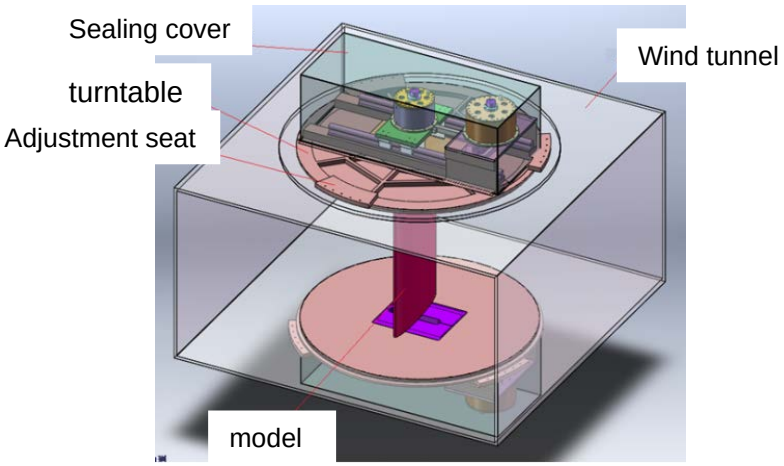

Figure1 Model driven system

The dynamic sensor adopts the XCQ-093 and XCS-093 series differential pressure sensor with temperature compensation and high sensitivity produced by American Kulite Company. 32 dynamic pressure sensors are installed in the mounting holes of the airfoil model, which flush with the surface of the airfoil model. The angle of attack is measured by an absolute rotary encoder produced by HEIDENHAIN Company of Germany.

2.2 Test methods and data processing

In this test, the dynamic pressure measuring test was carried out on the NACA0012 airfoil model with chord lengths of 500mm, 700mm and 900mm under the conditions of Reynolds number $\mathrm{Re}=1.5\times10^{6}$, average angle of attack 10° , amplitude 10° , and reduced frequency of *k*=0.03, 0.05 and 0.07. The model is installed vertically between the upper and lower walls. The drive system drives the airfoil model to do sinusoidal pitching oscillation motion, and the motion law of the angle of attack is $\alpha=10°+10°\sin(2\pi ft)$. An angle sensor is installed on the rotating shaft of the airfoil test model to measure the instantaneous angle of oscillation of the airfoil. During the test, the pressures of 32 dynamic pressure sensors installed on the upper and lower surfaces of the airfoil at mid-span are collected by the VXI acquisition system to calculate the airfoil's lift, differential pressure drag and pitching moment around the 1/4 chord line.

The instantaneous pressure coefficient on the surface when the airfoil model moves is calculated with the formula (1),

$$C_{P_i}(t)=\frac{P_i(t)-P_\infty}{q_\infty} \tag{1}$$

In the formula, P_∞ is the static pressure of the wind tunnel, q_∞ is the dynamic pressure of flow, P_i are the pressures of 32 dynamic pressure sensors. the airfoil surface pressure coefficient at each time *t*, is integrated using equations (2)-(4) to obtain the normal force, the chord force coefficient and the pitching moment coefficients of the airfoil around the 1/4 chord,

$$C_N(t) = \oint_s C_{pi}(t)\,d\bar{x} \tag{2}$$

$$C_t(t) = \oint_s C_{pi}(t)\,d\bar{y} \tag{3}$$

$$M_{z,1/4}(t) = \oint_s \bar{x} C_{pi}(t)\,\mathrm{d}\,\bar{x} + \oint_s \bar{y} C_{pi}(t)\,\mathrm{d}\,\bar{y} + C_N(t)/4 \tag{4}$$

where, $\bar{x}, \bar{y}$ represent the ratio of the pressure measuring point coordinates x, y to the airfoil chord length c, respectively. Record the airfoil angle of attack at each moment *t*, formulas (5) and (6) are applied to transform the force and moment coefficients of the body axis coordinate system to the wind axis coordinate system, and obtain the lift and pressure drag coefficients with the instantaneous angle of attack when the airfoil model oscillates.

$$C_y(t) = C_N(t)cos\alpha(t) - C_t(t)sin\alpha(t) \tag{5}$$

$$C_x(t) = C_N(t)sin\alpha(t) + C_t(t)cos\alpha(t) \tag{6}$$

Finally, the data of multiple periods are averaged according to formulae (7)-(9), and the average lift and the pressure drag coefficients and the pitching moment coefficient around the 1/4 chord are obtained,

$$\widetilde{C}_y = \frac{1}{N+1}\sum_{n=0}^{N} C_y(t+nT), 0 \le t \le T \tag{7}$$

$$\widetilde{C}_x = \frac{1}{N+1}\sum_{n=0}^{N} C_x(t+nT), 0 \le t \le T \tag{8}$$

$$\widetilde{M}_{z1/4} = \frac{1}{N+1}\sum_{n=0}^{N} M_{z1/4}(t+nT), 0 \le t \le T \tag{9}$$

where, T is the period of airfoil oscillation, $N+1$ is the total number of period.

The lift coefficient, the pressure drag coefficient and the pitching moment coefficient around the 1/4 chord without wall interference (nominal chord length is 0) are obtain by linear interpolation of test results of the 500mm chord model and the 900mm chord model. The wall interference correction is evaluated and corrected. The interpolation results of the 700mm chord length model are obtained in a similar way.

2.3 Test Results and Analysis

Figures 2 and 3 are the dynamic pressure measuring experimental results of the NACA0012 airfoil model with chord lengths of 500mm, 700mm and 900mm when *k*= 0.03 and 0.07 respectively, and the results of the chord length 700mm model obtained by interpolating the chord length 500mm and 900mm model experimental results. The Reynolds numbers are $Re = 1.5\times10^6$. The drive system drives the airfoil model to do sinusoidal pitching oscillation motion, and the motion law of the angle of attack is $\alpha = 10° + 10°\sin(2\pi ft)$.

It can be seen from Figure 2 that when the airfoil is subjected to the dynamic motion in the wind tunnel, due to the formation, development, break and recovery of the dynamic stall vortex, the shape of the airfoil aerodynamic characteristic curve forms a hysteresis loop. At the same time, because the existence of the wind tunnel wall increases the velocity of the flow field around the model, the lift coefficient of the airfoil increases. The larger the airfoil model (that is, the greater the blocking degree), the greater the lift coefficient. With the increase of the chord length of the model, the maximum drag coefficient basically increases, and the minimum value of the pitching moment coefficient becomes smaller.

It can be seen from Figure 3 that when other experiment conditions remain unchanged, only the reduced frequency increases as k=0.07, the lift coefficient of the airfoil increases, the maximum drag coefficient increases, and the minimum of the pitching moment coefficient becomes the smaller. The dynamic stall is delayed, and the scope of the hysteresis loop for lift and pitching moment also becomes larger. With the increase of the model chord length, the changing law of lift coefficient, drag coefficient and pitching moment coefficient is consistent with the reduced frequency k=0.03.

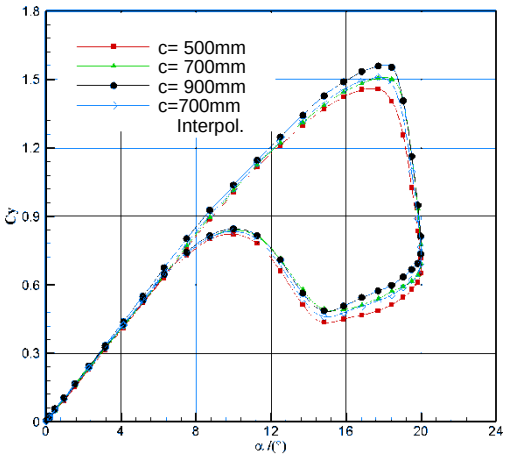

(a) lift coefficient

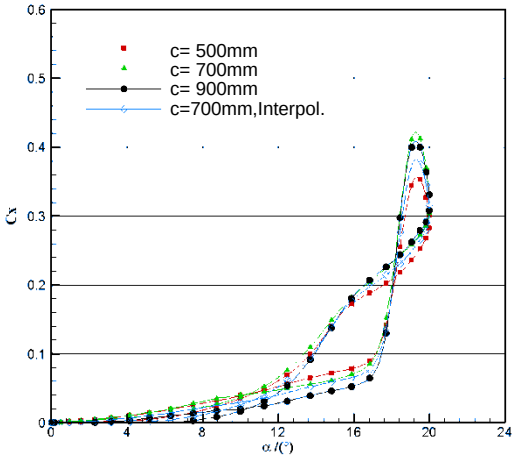

(b) drag coefficient

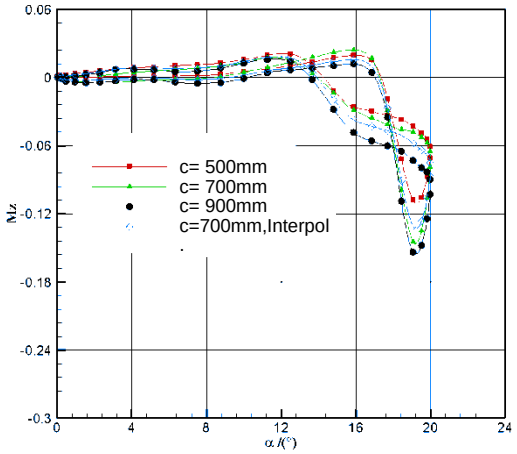

(c) pitching moment

Figure 2 Comparison between experimental results and interpolation results of 700mmm chord length model, k=0.03

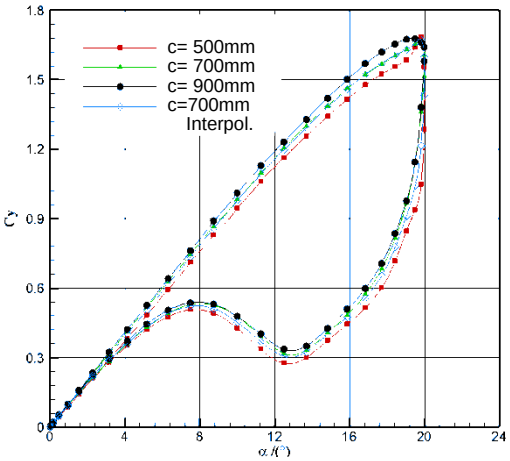

(a) lift coefficient

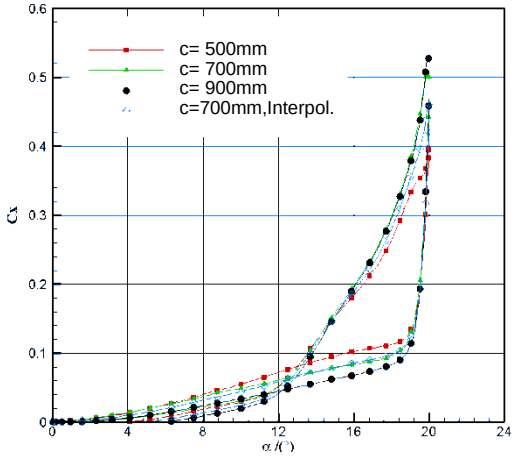

(b) drag coefficient

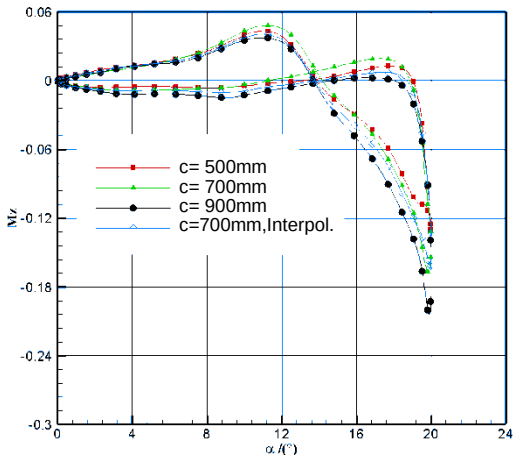

(c) pitching moment

Figure 3 Comparison between experimental results and interpolation results of 700mmm chord length model, k=0.07

It can also be seen from Figure 2 and Figure 3 that the experimental results of the 700mm chord model basically coincide with the results of the chord length 700mm model obtained by interpolation of the chord length 500mm and 900mm model experimental results, indicating that at the same dimensionless dynamic experimental parameter, it is feasible to obtain the force coefficients of other scale models by interpolating the dynamic experimental results of models of different sizes with geometric similarity.

Figure 4 and Figure 5 are the results of dynamic pressure measuring test of NACA0012 airfoil model with chord lengths of 500mm, 700mm and 900mm and the results without wall interference(Nominal chord length is 0mm) obtained by interpolating the test results with chord lengths of 500mm and 900mm when *k* = 0.03 and 0.07 respectively. The Reynolds numbers are $Re = 1.5 \times 10^6$, and the model performs pitching oscillation motion according to $\alpha = 10° + 10° \sin(2\pi ft)$.

It can be seen that the interpolated aerodynamic performance curves without wall interference are consistent with the experimental results of the chord lengths of 500mm, 700mm and 900mm with the change of the chord length of the test model. With the increase of the model chord length, the hysteresis loops of the lift and pitching moment coefficients become lager, the lift coefficient increases, the maximum drag coefficient basically increases, and the minimum value of the pitching moment coefficient is smaller.

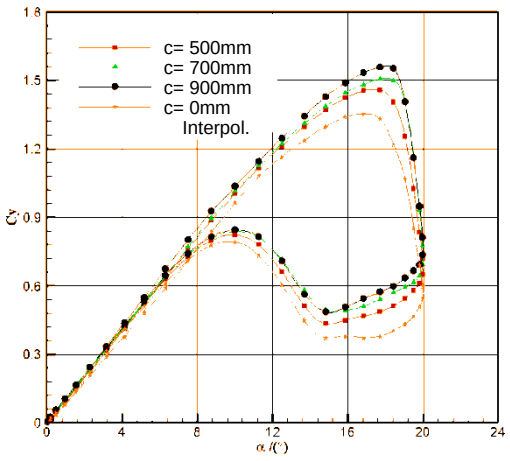

(a) lift coefficient

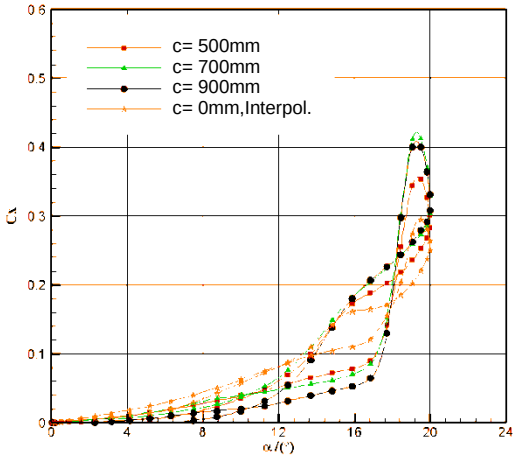

(b) drag coefficient

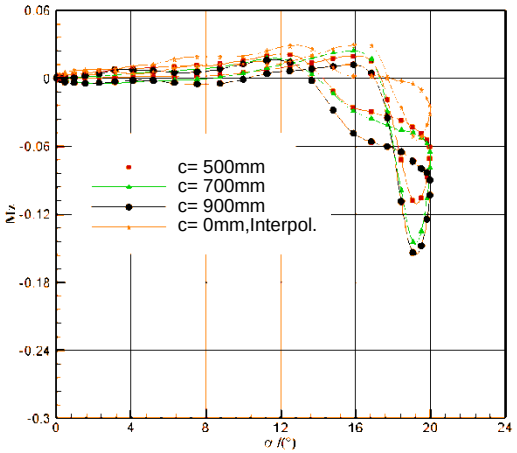

(c) pitching moment

Figure 4 Comparison between experimental results and interpolation results without wall interference (0 mm chord length), k=0.03

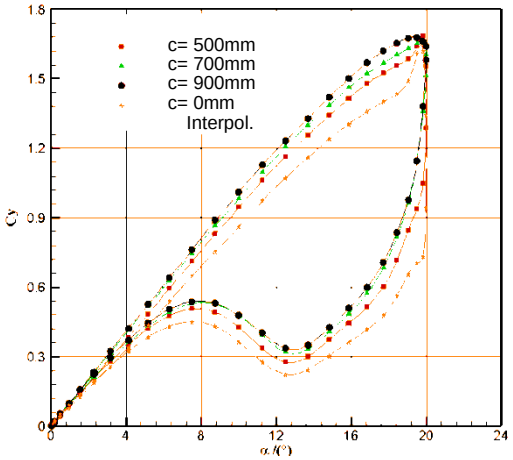

(a) lift coefficient

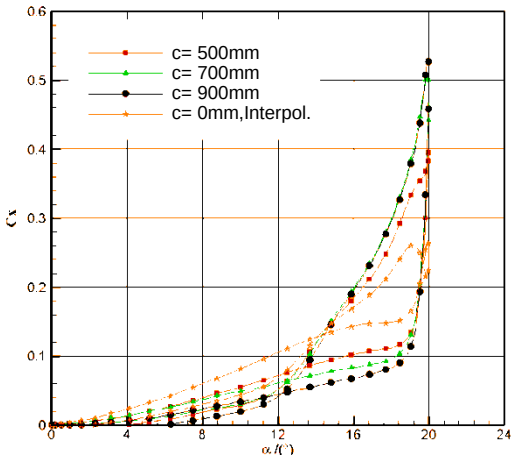

(b) drag coefficient

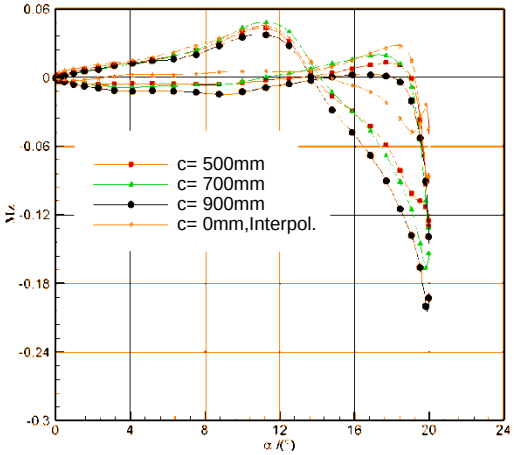

(c) pitching moment

Figure 5 Comparison between experimental results and interpolation results without wall interference (0 mm chord length), k=0.07

3. Numerical Research

3.1 Governing equation

In order to simulate the flow around the airfoil, the whole flow field is regarded as compressible and

viscous flow, and the coordinate system is established at the leading edge of the airfoil. The governing equation adopts the integral form of the unsteady Reynolds Average Navier-Stokes (RANS) equation (14).

$$\frac{\partial}{\partial t}\iint_{V} \boldsymbol{W} dV + \oint_{\delta V} \boldsymbol{F}\cdot \boldsymbol{n} dS = \oint_{\delta V} \boldsymbol{F}_{v}\cdot \boldsymbol{n} dS \tag{10}$$

where,

$$\boldsymbol{W} = \begin{bmatrix} \rho \\ \rho u \\ \rho v \\ \rho E \end{bmatrix} \tag{11}$$

$$\boldsymbol{F} = \begin{bmatrix} \rho(\boldsymbol{q}-\boldsymbol{q_b}) \\ \rho u(\boldsymbol{q}-\boldsymbol{q_b}) + p\boldsymbol{I}_x \\ \rho v(\boldsymbol{q}-\boldsymbol{q_b}) + p\boldsymbol{I}_y \\ \rho H(\boldsymbol{q}-\boldsymbol{q}_b) + p\boldsymbol{q}_b \end{bmatrix} \tag{12}$$

$$\boldsymbol{F_v} = \begin{bmatrix} 0 \\ \boldsymbol{\tau_{xx}}\boldsymbol{I}_x + \boldsymbol{\tau_{xy}}\boldsymbol{I}_y \\ \boldsymbol{\tau_{xy}}\boldsymbol{I}_x + \boldsymbol{\tau_{yy}}\boldsymbol{I}_y \\ f\boldsymbol{I}_x + g\boldsymbol{I}_y \end{bmatrix} \tag{13}$$

where, f and g respectively defined as

$$f = u\tau_{xx} + v\tau_{xy} + k\frac{\partial T}{\partial x} \tag{14}$$

$$g = u\tau_{yx} + v\tau_{yy} + k\frac{\partial T}{\partial y} \tag{15}$$

where V is the volume of the control volume, S is the surface of the control volume, $\boldsymbol{W}$ is a vector of conserved variables, $\boldsymbol{F}$ and $\boldsymbol{F}_v$ are the convective flux vector and viscous flux vector respectively, n is the normal unit vector outside the boundary of the control volume, ρ is the fluid density, $\boldsymbol{q}$ is the fluid velocity vector, $\boldsymbol{q}_b$ is the grid velocity vector, k is the heat transfer coefficient, T is the fluid temperature, E is the total energy, and H is the total enthalpy.

To close the N-S equation, introduce the equation of state

$$p = (\gamma-1)\left[\rho E - \frac{1}{2}\rho(u^2+v^2)\right] \tag{16}$$

where for ideal gas, specific heat ratio $\gamma = 1.4$, $\rho = 1.225$.

3.2 Numerical simulation method

The governing equations are spatially discretized using the finite volume method of the center format(15). The dual-time advancing method proposed by (16) is used for unsteady calculations. The multi-step Runge-Kutta format(17) is used for pseudo-time advancement, and the accelerated convergence techniques such as local time step, implicit residual smoothing, and multi-grid are used（18）. The turbulence model used in this paper is the shear stress transport $k-\omega$ model, referred to as the $k-\omega$ SST model, which is a two-equation turbulence model (19).

3.3 Boundary conditions

The boundary conditions for numerical simulation are set as：

(1) Wall boundary conditions: The boundary conditions on the airfoil model surface and the upper and lower walls of the wind tunnel satisfy the no slip boundary condition.

(2) Far-field boundary conditions: In the numerical simulation of free air flow, this paper uses the one-dimensional Riemann invariant (20) to deal with the far-field non-reflective boundary conditions.

(3) Entrance and exit boundary conditions: When numerical simulation of wind tunnel flow field is carried out, the entrance is set as the velocity inlet boundary condition, that is, the free air velocity V_∞ at infinity is set as the velocity at the entrance of the calculation zone. It is set as the pressure outlet boundary condition to define the static pressure of the flow outlet.

3.4 Calculation Grid

Geometric model: The numerical simulation of the wind tunnel flow uses the same calculation domain as the NF-3 low-speed wind tunnel of Northwestern Polytechnical University. The wind tunnel test section is 8 meters long, 3 meters wide and 1.6 meters high. The moment center of the airfoil model is 1⁄4 chord length point, and the moment center is located 3.6 meters from the entrance of the wind tunnel test section. In the free air numerical simulation, the outer boundary size of mesh around the airfoil is 20 times the chord length of the airfoil model.

The motion chimera grid system used consists of two sets of grids: one is the C-grid generated for the airfoil, and the other is the H-grid generated for the background. Background mesh hole cell recognition, contribution cell search, and information transfer between chimera grids are carried out. Information transfer between chimera grids is achieved through bilinear interpolation. The generated chimera grid is shown in Figure 6.

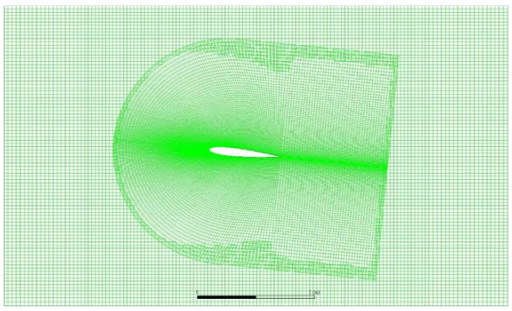

Figure 6 Chimera grids

3.5 Tunnel wall interference calculation method

The calculation of the wall interference is divided into two steps. Firstly, the numerical simulations of the flow field around the models in the wind tunnel flow field and in the free air field using the Navier-Stokes equation are carried out, in the same Mach number Ma, Reynolds Number Re, Strouhal number S_r and the angle of attack α. The boundary conditions are set for wind tunnel flow chimera grid, the numerical simulation is carried out, and the aerodynamic force and moment coefficients of the airfoil model in the wind tunnel are calculated. Then the boundary conditions are set for free air chimera grid, the numerical simulation is carried out, and aerodynamic force and moment coefficients of the airfoil in the free air are calculated. The difference between the two results is the amount of the wind tunnel wall interference. The calculation formula of the influence amount (18) is

$$\Delta C_l = C_{l,tunnel} - C_{l,free} \tag{17}$$

$$\Delta C_d = C_{d,tunnel} - C_{d,free} \tag{18}$$

$$\Delta C_m = C_{m,tunnel} - C_{m,free} \tag{19}$$

The corrected aerodynamic test data can be obtained by subtracting the corresponding amount of wind tunnel wall interference from the results of the wind tunnel test, namely,

$$C_{l,correction} = C_{l,test} - \Delta C_l \tag{20}$$

$$C_{d,correction} = C_{d,test} - \Delta C_d \tag{21}$$

$$C_{m,correction} = C_{m,test} - \Delta C_m \tag{22}$$

where C_l, C_d and C_m are lift, drag and moment coefficients, respectively. The subscript *free* and subscript *tunnel* indicate the aerodynamic force and moment coefficients of the airfoil in free air and in the wind tunnel flow field obtained by numerical simulation, respectively. And the subscript *test* and subscript *correction* indicate the aerodynamic force and moment coefficients of the airfoil of the wind tunnel test and corrective respectively.

3.6 wall interference correction of Unsteady Airfoil test

3.6.1 Test model

The wind tunnel test in Guilmineau described by (21) was used for research on evaluation and correction of wall interference of the unsteady airfoil test. The test model uses the NACA0012 airfoil with a chord length of 610 mm and a spanwise length of 1600 mm.

3.6.2 Airfoil movement

The variation of the angle of attack of the NACA0012 airfoil with a 1/4 chord point for pitching oscillation is

$$\alpha(t) = \alpha_0 + A \times \sin(2\pi\omega t) \tag{23}$$

where t is the physical time and it's step of the time direction advance in the calculation is $\Delta t = 0.001s$, $a(t)$ is the instantaneous angle of attack of the airfoil, a_0 is the average angle of attack of the airfoil, A is the amplitude of the airfoil angle of attack, ω is the frequency of the pitching oscillation and given by the reduced frequency k,

$$k = \frac{\pi\omega c}{v} \tag{24}$$

where π is circumference ratio, v is the airflow speed and c is the chord of airfoil. The reduced frequency k reflects the interaction between the main flow motion around the airfoil and the oscillating pitching motion of airfoil around the rotating point. Its value characterizes the magnitude of the effect of oscillatory motion on main flow motion.

The airflow speed is given by the Reynolds number:

$$Re = \frac{\rho v c}{\mu} \tag{25}$$

where μ is the molecule viscosity coefficient of the air, ρ is the air density.

3.6.3 Wall interference correction results of airfoil unsteady test

The parameter values in formula (23) for this research are $\alpha_0 = 15°$, $A = 10°$, $Re = 1.0 \times 10^6$ and $k = 0.15$. The correction results of wind tunnel test data based on the numerical simulation correction method are compared with the uncorrected test data in Figure 7.

The results show that under the same instantaneous angle of attack, for the ascending process(upstroke), the modified lift coefficient C_l and the drag coefficient C_d are slightly smaller than the uncorrected results, the moment coefficient C_m is slightly larger than the uncorrected result, and the differences between the corrected and uncorrected aerodynamic force and moment coefficients of the airfoil in the descending process(downstroke) are very small. And in a motion loop, the wall interference correction increases with the increase of the angle of attack, that is, the greater the instantaneous angle of attack, the greater the influence of the wind tunnel wall on the airfoil aerodynamic coefficients. This is consistent with the law of wind tunnel wall interference. It is shown that the proposed method for correcting the wind tunnel wall interference in the airfoil unsteady wind tunnel is feasible and effective based on the motion chimera grids.

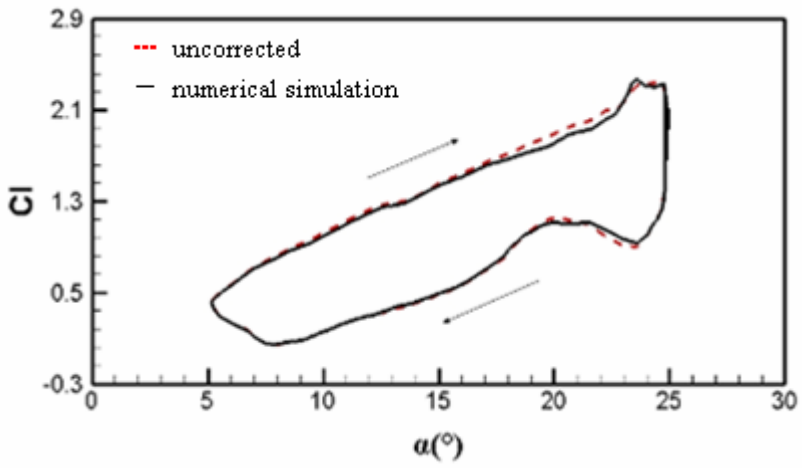

(a) Lift coefficient

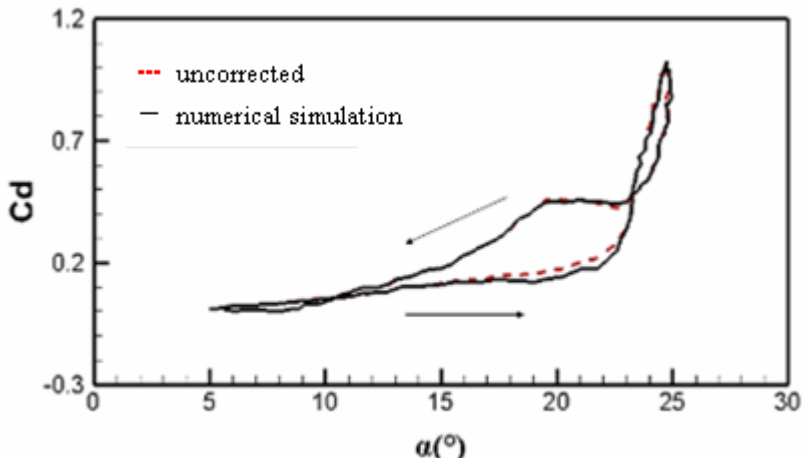

(b) Drag coefficient

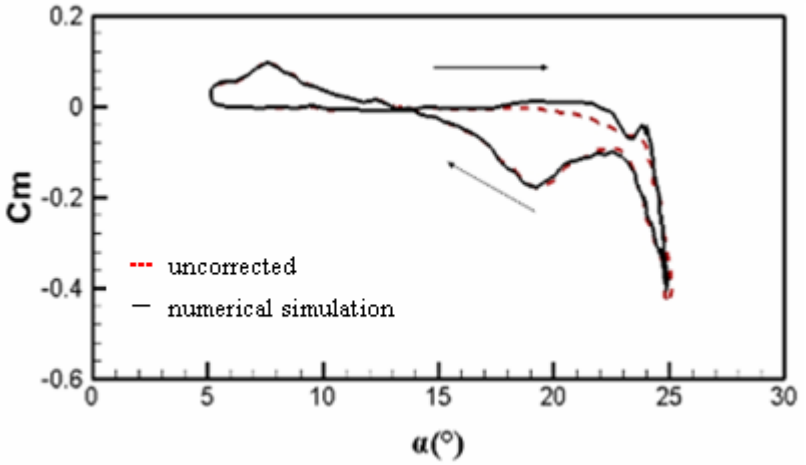

(c) Pitching moment coefficient

Figure 7 Results of airfoil unsteady test with and without wall interference correction

In order to better understand the flow characteristics at instantaneous angle of attack in an oscillation pitching period, as well as the formation, development, the process of propagating along the upper surface of the airfoil and eventually falling off of dynamic stall vortexes, the streamline pattern in figure 8 and 9 show the flow around the airfoil at different times.

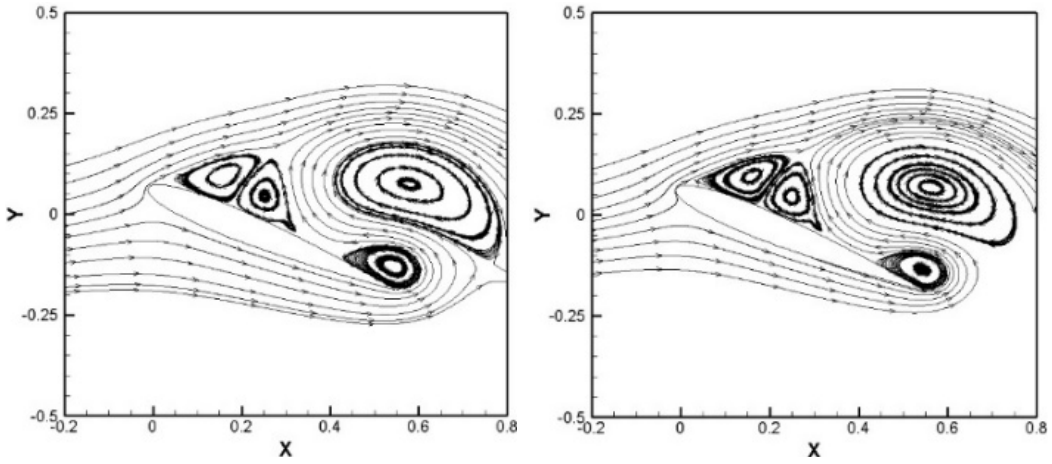

(a) Wind tunnel flow field (b) Free air

Figure 8 $\alpha(t) = 24.2°$ upstroke flow pattern

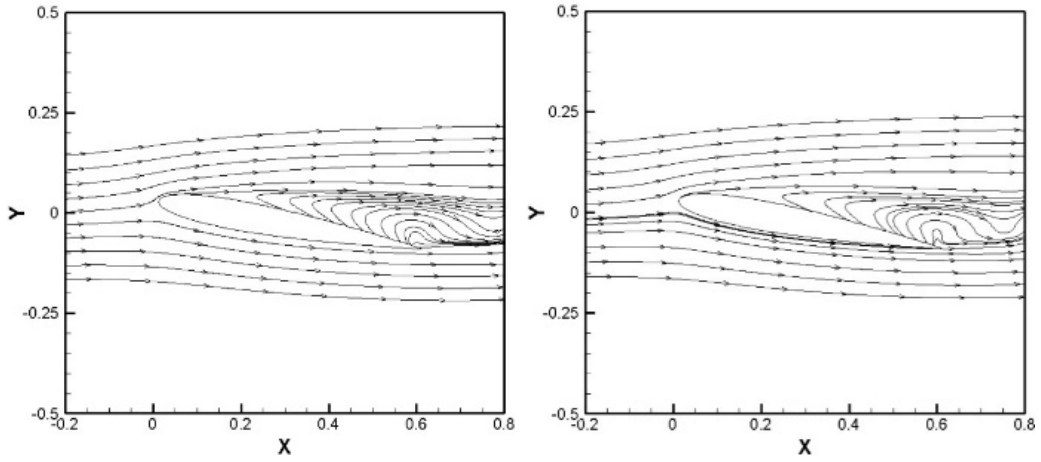

(a) Wind tunnel flow field (b) Free air

Figure 9 $\alpha(t) = 11.37°$ downstroke flow pattern

The above calculated flow pattern comparison shows that the airfoil flow structure in the wind tunnel flow is consistent with and similar to that in the free air flow. In the air flow around the airfoil, many small-scale vortexes are formed and gradually fall off, indicating that the existence of wind tunnel wall does not change the basic structure of the flow around airfoil, providing a basis for further exploration of the simplified wall interference correction method.

4. Conclusion

Based on the two methods of experiment and numerical simulation, the wall interference of airfoil dynamic experiment is studied. The main conclusions are as follows:

(1) Experimental method and Numerical simulation correction method are easy to implement and give correct results, but are not easy to use in usual experiments.

(2) The experimental correction method that the tunnel wall interference of the airfoil dynamic test is obtained through wind tunnel experiments with three different scale models and the same dimensionless motion parameters can correctly evaluate and correct the unsteady tunnel wall interference.

(3)The Navier-Stokes equations numerical simulation method based on the dynamic chimera grids can simulate the flow of the airfoil model well in the wind tunnel and under free flow conditions. The correction method for the wall interference of the airfoil dynamic wind tunnel test based on this numerical simulation is correct and feasible.

(4) The existence of the wind tunnel wall does not change the flow structure around the airfoil during the oscillating pitching motion, providing a basis for further exploration of the simplified correction method.

5. Contact Author Email Address

mailto: jiaoyuqin@nwpu.edu.cn

6. Copyright Statement

References

[1] Oshima R, Sawada H and, Obayashi S. A Development of Dynamic Wind Tunnel Testing Technique by Using a Magnetic Suspension and Balance System. *54th AIAA Aerospace Sciences Meeting*, 2016.

[2] Mokhtar W and Britcher C. Boundary interference assessment and correction for open test section wind tunnels using panel methods. *42nd AIAA Aerospace Sciences Meeting and Exhibit*, pp609, 2004.

[3] Dančová P, Haque A U and Asrar W, et al. Comparison of data correction methods for blockage effects

in semispan wing model testing. *EPJ Web of Conferences*, pp114, 2016.

[4] Soltani M R, Marzabadi F R and Mohammadi Z. Experimental Study of the Plunging Motion with Unsteady Wind Tunnel Wall Interference Effects. *Experimental Techniques*, Vol.36, No.5, pp30-45, 2012.

[5] Jin J, Ren X and Gao C, et al. Analysis of the Effects of Wall Interference on 0.4×0.8-Meter Transonic Wind Tunnel Airfoils Tests. *51st AIAA Aerospace Sciences Meeting including the New Horizons Forum and Aerospace Exposition*, 2013.

[6] General Theory of Aerodynamic Instability and the Mechanism of Flutter. NACA Report 496, 1935.

[7] Gordon L J. Principles of helicopter aerodynamics. *Cambridage Aerodynamic Series*, 2000.

[8] Possio C. L'azione aerodinamica sul profilo oscillante in un fluido compressibile a velocita iposonora. *L'aerotecnica*, Vol.18, No.4, pp 441-458, 1938.

[9] Bland S R. The two-dimensional oscillating airfoil in a wind tunnel in subsonic flow. *SIAM Journal on Applied Mathematics*, Vol.18, No.4, pp830-848, 1970,.

[10]Fromme J and Golberg M. Computation of aerodynamic interference effects on oscillating airfoils with controls in ventilated subsonic wind tunnels. *17th Aerospace Sciences Meeting*, pp346, 1979.

[11]Ding K, Zhang W and Li Z, et al. Study on tunnel wall interference in unsteady pressure measurement experiment of large pitching motion of delta wing(in Chinese). *Journal of Aerodynamics*, No.3, pp330-335, 2000.

[12]Huang D, Li Z and Ding K, et al. Experimental study on unsteady wall interference with large pitch motion of delta wing(in Chinese). *Journal of Nanjing University of Aeronautics and Astronautics*, No.01, pp13-17, 2003.

[13]Li G, Zhang W and Huang X, et al. Study on the wall effect of airfoil dynamic wind tunnel test(in Chinese). *Engineering Mechanics*, Vol.36, No.08, pp235-247, 2019.

[14]Yan C. *Computational Fluid Dynamics Method and Application(in Chinese)*. Beijing University of Aeronautics and Astronautics Press, Beijing, 2006.

[15]Jameson A. Schmidt W and Turkel F. Numerical solutions of the Euler equations by finite volume methods using Runge-Kutta time stepping schemes. *American Institute of Aeronautic and Astronautics*, AIAA 81-1259,1981.

[16]Jameson A.Time dependent calculations using multigrid, with applications to unsteady flows past airfoils and wings. *American Institute of Aeronautic and Astronautics*, AIAA 91-1596,1991.

[17]Wang C. Analytical method and experimental study of aerodynamic characteristics of micro rotor. *Nanjing University of Aeronautics and Astronautics*, Nanjing, 2010.

[18]Jiao Y Q, Qiao Z D. Numerical Simulation of Overseting Mesh Viscous Flow for Wind Tunnel Wall Interference(in Chinese). *Journal of Experimental Fluid Mechanics*, Vol.16, No.1, pp 43-49,2002,.

[19]Menter F R. Zonal two-equation model k-ω models for aerodynamic flows. *24th Fluid Dynamics Conference*, Orlando, Florida, 1993.

[20]Singh K P. Unstructured method for flows past bodies in general three dimensional relative motion. *AIAA Journal,* Vol.39, No.2, pp 219-224, 2001.

[21]Guilmineau E, Piquet J, Queutey P. Unsteady two-dimensional turbulent viscous flow past aerofoil. *International Journal for Numerical Methods in Fluids*, Vol.25, No.3, pp315-366*,* 1997.